The low-field remanent magnetization of the disordered antiferromagnets $K_2Fe_{1-x}In_xCl_5.H_2O$ and $K_2Fe(Cl_{1-x}Br_x)_5.H_2O$

1994 J. Phys.: Condens. Matter 6 5725

(http://iopscience.iop.org/0953-8984/6/29/015)

J. Phys.: Condens. Matter 6 (1994) 5725–5740. Printed in the UK

The low-field remanent magnetization of the disordered antiferromagnets $K_2Fe_{1-x}In_xCl_5 \cdot H_2O$ and $K_2Fe(Cl_{1-x}\ Br_x)_5 \cdot H_2O$

C C Becerra†, A Paduan-Filho†, T Fries‡, Y Shapira‡ and F Palacio§

† Instituto de Física, Universidade de São Paulo, CP 20516, São Paulo S P, Brazil

‡ Department of Physics, Tufts University, Medford, MA 02155, USA

§ Instituto de Ciencia de Materiales de Aragon, CSIC, Universidad de Zaragoza, E-50009, Zaragoza, Spain

Received 21 January 1994

Abstract. Magnetization measurements on single crystals of the site-diluted easy-axis antiferromagnet $K_2Fe_{1-x}In_xCl_5 \cdot H_2O$ were carried out at very low magnetic fields applied along the easy axis. The data reveal that a remanent magnetization M_r develops below the Néel temperature T_N. This remanent magnetization is parallel or nearly parallel to the easy axis. For all concentrations x studied, $0.03 \leqslant x \leqslant 0.14$, the sign and magnitude of $M_r(T)$ in a given sample and for a given temperature are governed only by the axial field (H_{axial}) present when cooling through T_N. The remanent magnetization is observed in fields as low as 10^{-3} Oe. For a given H_{axial}, M_r increases with decreasing T. At a given T, M_r versus H_{axial} is very nearly saturated even at ~ 1 Oe. The magnitude of the saturated remanent moment increases with x in the range of x studied. The normalized remanent magnetization $M_r(t)/M_r(0)$, where $t = T/T_N$ is the reduced temperature, follows a universal curve, i.e., it is independent of H_{axial} for a given sample (in fields up to several oersted), and it is also the same for all $K_2Fe_{1-x}In_xCl_5 \cdot H_2O$ samples. Moreover, the t dependence of $M_r(t)/M_r(0)$ in $K_2Fe_{1-x}In_xCl_5 \cdot H_2O$ is the same as in $Mn_{1-x}Zn_xF_2$. Values for the effective critical exponent β_r, obtained from the temperature dependence of M_r close to T_N, are close to 0.4. (The extrapolated values at T_N are between 0.35 and 0.39.) Temperature cycles following cooling through T_N in zero field, and isothermal field cycles below T_N, suggest that a domain-like structure is obtained when the sample is cooled in zero field through T_N. Magnetization measurements were also carried out on the random-bond system $K_2Fe(Cl_{1-x}Br_x)_5 \cdot H_2O$ with $x \cong 0.25$. A remanent moment also develops in this case, but it is two orders of magnitude smaller than in the site-diluted system. The temperature dependence of M_r is also distinct in this case: with decreasing T, M_r first increases but then decreases. The mechanism that causes the low-field remanent magnetization is yet to be fully identified. The effect cannot be attributed to random fields (i.e., the excess magnetization of random-field-induced domains) because M_r saturates at very low fields. Domains that exist even in the absence of random fields are a likely source for the low-field remanent magnetization, but the details are still unclear. An explanation based on the volume effect, due to the statistical imbalance between the numbers of up and down spins in each of the domains, which exist even in the absence of random fields, seems to fail. Domain-wall magnetization, and domain magnetization due to the piezomagnetic effect, are other possibilities that remain to be explored. Domain formation may be facilitated by non-magnetic cations that act as vacancies in the magnetic lattice; this may be the reason why M_r in $K_2Fe_{1-x}In_xCl_5 \cdot H_2O$ is much larger than that in $K_2Fe(Cl_{1-x}Br_x)_5 \cdot H_2O$.

1. Introduction

Recent magnetization measurements on disordered easy-axis antiferromagnets at very low magnetic fields H [1–3] revealed that below their Néel temperature T_N these systems exhibit

a remanent magnetization M_r along the easy axis. This M_r depends on the axial component of H (along the easy axis) present when the sample is cooled through T_N. The remanent moment is observed in axial fields as low as 10^{-3} Oe. Saturation of M_r occurs even at ~ 1 Oe. This type of behaviour in disordered antiferromagnets has never been reported before, to our knowledge.

Dilute uniaxial antiferromagnets have been the focus of attention in recent years primarily because of their connection to the random field Ising model (RFIM). The dilute antiferromagnet in a magnetic field (DAFF) is a physical realization of the RFIM [4]. A dilute antiferromagnet exhibits a long-range order (LRO) if it is cooled from above T_N in zero magnetic field (ZFC). If the cooling from above T_N occurs in the presence of a magnetic field along the easy axis (FC procedure) then a metastable microdomain structure is obtained [5–7]. This is due to the extremely slow dynamics involved, which prevent the system from establishing LRO. The characteristic size of the domain depends in the random field (RF) present when the sample is cooled through T_N. Experimentally, an excess magnetization $\Delta M = M_{FC} - M_{ZFC}$ (i.e., the difference between the FC and ZFC magnetizations, measured at the same T and H) was observed in several materials [8–10]. The magnitude of ΔM has been related to the mean radius R of these RF-induced domains. Excess magnetization and domain structures have also been obtained in Monte Carlo simulations of the dilute Ising antiferromagnet [11–13]. Although the remanent magnetization observed in the present work may also be related to domains, it seems to have no relation to the domains caused by the RF induced by H. That is, the relevant domains exist even at zero (or very low) magnetic field.

In this paper we present more extensive results for the low-field magnetic properties of the disordered antiferromagnets $K_2Fe_{1-x}In_xCl_5{\cdot}H_2O$ and $K_2Fe(Cl_{1-x}Br_x)_5{\cdot}H_2O$. Extensive results on the disordered system $Mn_{1-x}Zn_xF_2$ have already been reported [3].

2. Experimental details

The compounds with the general formula $X_2YZ_5{\cdot}H_2O$, where X=K or Rb, Y=Fe or In and Z=Cl or Br, are isomorphous and have an orthorhombic structure belonging to the *Pnma* space group. The Fe compounds are low-anisotropy antiferromagnets [14]. Substitutions of In for Fe, or of Br for Cl, are possible. Such substitutions allow studies of the magnetic properties of 'random-site' and 'random-bond' antiferromagnets, respectively.

Single crystals of $K_2Fe_{1-x}In_xCl_5{\cdot}H_2O$ ($x = 0.03$, 0.10, 0.11 and 0.14) and $K_2Fe(Cl_{1-x}Br_x)_5{\cdot}H_2O$ ($x \cong 0.25$) were grown from appropriate aqueous solutions of KCl, $InCl_3$, $FeCl_3 \cdot 6H_2O$ and KBr. No difference was observed between large and small crystals grown from the same starting solution. The concentration x in the crystals was obtained from the Curie–Weiss constant, which was determined from the susceptibility at temperatures well above T_N. Once a curve for T_N versus x was obtained, we occasionally used the measured T_N as an indication of the concentration x in the crystal. We estimate an accuracy of 10% for the values of x. All samples used in the magnetization measurements had linear dimensions of several millimetres.

Most magnetization measurements were made using a vibrating sample magnetometer (VSM). The remaining data were taken using a superconducting quantum interference device (SQUID) magnetometer manufactured by Quantum Design. Superconducting magnets were used with both set-ups. All samples were mounted with the easy axis (axial direction) along the bore of the superconducting magnet. Most data were for the axial (longitudinal) component of the magnetization, although occasionally the transverse component was also

measured. Because the remanent magnetization turned out to be an extremely sensitive function of H, it was essential to avoid trapped flux in the superconducting magnet. For this purpose, the magnet with its leads open was cooled from above the superconducting transition temperature before each experimental run. The residual field, less than ~ 1 Oe, was then due to the Earth field as distorted by the local environment (laboratory equipment, steel beams in walls, etc). In low-field experiments with the VSM set-up the axial field was generated by an auxiliary coil, coaxial with the magnet and mounted within its bore. A zero axial field at the sample was achieved by setting the current through the auxiliary coil to a value I_0 at which the remanent magnetization M_r in the sample reversed its sign. This procedure is discussed in subsection 3.1. The accuracy of setting $H_{axial} = 0$ was ± 0.003 Oe. Positive and negative axial fields, up to several oersted, were then generated with currents I that differed from I_0, with $H_{axial} \propto (I - I_0)$. The precision of setting H_{axial} was 0.001 Oe. Once all the data in fields up to several oersted were taken in a given experimental run, data at higher fields were obtained by using the superconducting magnet in the usual way. The procedures used to accurately control H_{axial} in the SQUID system, for fields up to several oersted, are described in [2] and [3].

3. Experimental results

3.1. Magnetization of $K_2Fe_{1-x}In_xCl_5{\cdot}H_2O$

The magnetization M along the easy axis was measured as a function of T at fixed values of H_{axial}. For each H_{axial} data were first taken while cooling in that field, starting from above T_N (FC procedure). A typical time interval between successive data points was 5 min for data near T_N, and 2 min at lower temperatures. For all $K_2Fe_{1-x}In_xCl_5{\cdot}H_2O$ samples at non-zero H_{axial} the axial magnetization rose dramatically when the temperature decreased through T_N. Subsequent heating of the sample at the same constant H_{axial} (FH procedure) revealed that the M against T curve at fixed H_{axial} is reversible. Figures 1 and 2 show typical FC results for $x = 0.03$ and $x = 0.14$, respectively. The FH data follow the same curves.

The striking rise of the axial magnetization below T_N is similar to that reported in $Mn_{1-x}Zn_xF_2$ [3]. In a control experiment on pure $K_2FeCl_5{\cdot}H_2O$, no rise of the magnetization below T_N (in comparable fields) was detected with the VSM system, with a resolution of 10^{-4} emu g^{-1}. Measurements of the transverse moment in the sample with $x = 0.10$, performed with the SQUID system, showed that any rise in the transverse moment was at least an order of magnitude smaller than that of the longitudinal (axial) moment at $H_{axial} \sim 0.1$ Oe. This result is significant since the transverse component of the Earth field (which was always present) was also of the order of 0.1 Oe. The same result was also obtained with the VSM system: the magnetization of the sample with $x = 0.11$ when it was mounted with the easy axis perpendicular to the bore was an order of magnitude smaller than that when the same sample was cooled with its easy axis along the bore. (In both cases the magnetization was measured along the bore.) Thus, the rise of the magnetization below T_N is confined to the axial magnetization component.

Examination of figures 1 and 2 indicates that the rise of the magnetization (below T_N) is already nearly saturated in axial fields as low as 1 Oe. This point is made more clearly in figure 3, which shows the dependence of M on the field H_{axial} in which the sample was cooled. These data are for $x = 0.11$ at 6 K. (The data collapse discussed below implies that the curve is the same at any T below T_N, except for the ordinate scale.) Most of the rise in the magnetization occurs for axial fields below 0.1 Oe. The inset shows the behaviour at

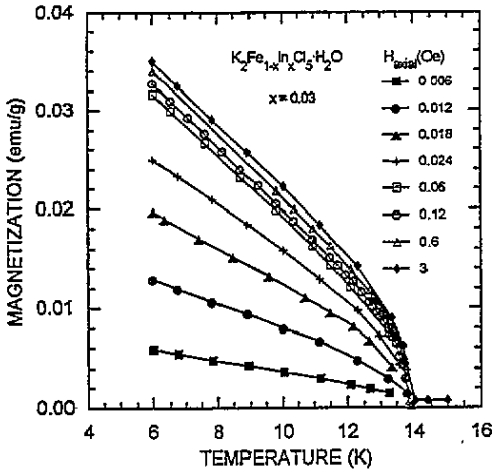

Figure 1. The temperature dependence of the magnetization for $x = 0.03$ at several axial magnetic fields. These are FC data, but FH data at the same fields show that these curves are reversible.

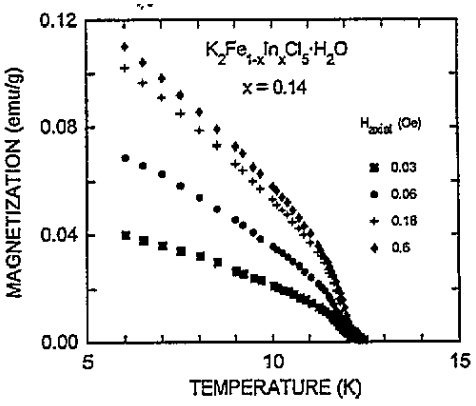

Figure 2. The temperature dependence of the magnetization for $x = 0.14$ at several axial fields. Only FC data are shown here (the FH results fall on the same curves.)

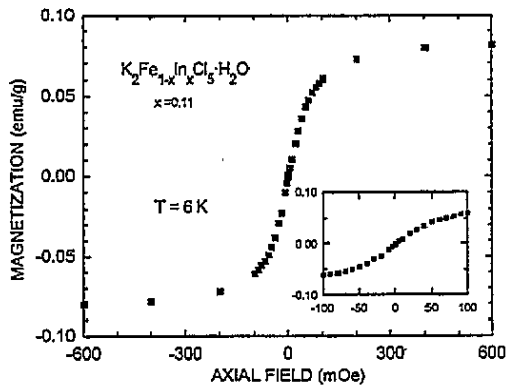

Figure 3. The dependence of M on the field H_{axial} in which the sample was cooled. These data are for $x = 0.11$ at $T = 6$ K. The inset shows an expanded view of the region between -0.1 and $+0.1$ Oe.

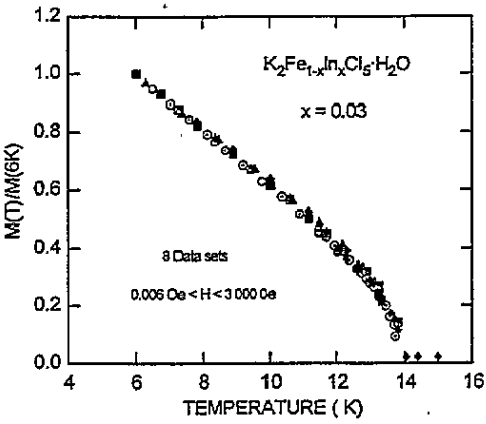

Figure 4. The temperature dependence of the normalized magnetization $M(T)/M(6\text{ K})$ for $x = 0.03$. All the eight data sets in figure 1 are included in this plot.

these low fields. The type of curve shown in figure 3 was used to find the current I_0 through the auxiliary coil at which H_{axial} was zero (see section 2). That is, we chose the current setting at which the magnetization well below T_N reversed its sign as that corresponding to zero axial field. This choice is discussed in [3].

The data in figures 1 and 2 are qualitatively similar to those for $Mn_{1-x}Zn_xF_2$ [3]. The rise of M below T_N implies that a remanent magnetization M_r develops when the sample enters the antiferromagnetic phase. One important quantitative difference between $K_2Fe_{1-x}In_xCl_5{\cdot}H_2O$ and $Mn_{1-x}Zn_xF_2$ is that the magnetization rise below T_N

in $K_2Fe_{1-x}In_xCl_5 \cdot H_2O$ (expressed in emu g^{-1}) is one to two orders of magnitude larger. On the other hand, the relevant susceptibility $\chi_\parallel$ per gram (for H along the easy axis) is comparable in both systems. Following [2] and [3] we express M as

$$M = \chi_\parallel H_{\text{axial}} + M_r. \tag{1}$$

The relative size of the two terms on the right-hand side (RHS) of (1) is different for $K_2Fe_{1-x}In_xCl_5 \cdot H_2O$ and $Mn_{1-x}Zn_xF_2$. As a result, the measured magnetization M below T_N and at $H \leqslant 1$ Oe is very nearly equal to M_r in the $K_2Fe_{1-x}In_xCl_5 \cdot H_2O$ system. We shall not distinguish between M and M_r in this system, except when $H_{\text{axial}} \gg 1$ Oe.

Figure 3 shows that M saturates below 1 Oe. The saturation value increases with the In concentration x, as already reported in [1]. Another noteworthy feature is the existence of a 'tail' near T_N in each of the curves of M against T for $x = 0.14$ (figure 2). This tail is presumed to arise from the broadening of the ordering transition by an inhomogeneity in the composition of the sample. No noticeable tail is observed in figure 1 for $x = 0.03$.

In some experiments H_{axial} was reduced isothermally to zero after the sample was cooled in a constant field to some temperature below T_N. The data showed that removing the field had a negligible effect on M. Moreover the magnetization at zero H_{axial} remained unchanged for periods longer than 1 h. Thus, the FC value of M (measured after cooling from above T_N in a constant H_{axial}) can be identified as the thermoremanent magnetization (TRM). Similar results were obtained in the $Mn_{1-x}Zn_xF_2$ system [3], except that the term $\chi_\parallel H$ had to be considered in that case.

3.2. *Data collapse for $K_2Fe_{1-x}In_xCl_5 \cdot H_2O$*

Analysis of figures 1 and 2 shows that for a given sample the various M against T curves at different H_{axial} differ only by a scale factor. That is, if the values of M on each curve are normalized to the value at one chosen temperature below T_N then all normalized curves are the same for a given sample. Such 'data collapse' is shown in figures 4 and 5. In figure 4 the eight data sets in figure 1, for $x = 0.03$ at $0.006 \text{ Oe} \leqslant H \leqslant 3$ Oe, have collapsed into a single curve after a normalization at 6 K. In figure 5 the four data sets in figure 2, for $x = 0.14$ at $0.03 \text{ Oe} \leqslant H \leqslant 0.6$ Oe, have collapsed into a single curve after a normalization at 6 K. It is remarkable that data collapse is obeyed even in the 'tail' region of figure 5. Data collapse in $Mn_{1-x}Zn_xF_2$ was discussed in [3].

As in the $Mn_{1-x}Zn_xF_2$ system, data sets for different x can be collapsed into a single curve by using the reduced temperature $t = T/T_N$ instead of T. Such data collapse for different x, for all values of H_{axial}, is achieved by normalizing each M against t curve (at constant field) to the value of M at a single t. An example of data collapse for both $x = 0.03$ and $x = 0.14$ is shown in figure 6. In the case of $x = 0.14$, for which the data exhibit a 'tail' near T_N, the value of T_N that enters the definition of t was chosen to be at the inflection point of M against T. The inset in figure 6 shows the result very near T_N. In this region the two samples exhibit different behaviours because the transition in one sample is much broader than that in the other. Otherwise, the two normalized data sets agree.

If the reduced temperature t is used then a still more general data collapse is obtained: the normalized magnetization in the $K_2Fe_{1-x}In_xCl_5 \cdot H_2O$ system agrees with that for $Mn_{1-x}Zn_xF_2$ samples. This more universal data collapse is illustrated in figure 7, which compares two data sets for the normalized magnetization in $K_2Fe_{1-x}In_xCl_5 \cdot H_2O$ ($x = 0.10$) with one of the normalized curves for $Mn_{1-x}Zn_xF_2$. As shown in [3] all normalized curves in the latter system collapse into a single curve, so that the full curve of figure 7 is representative of all normalized data for the $Mn_{1-x}Zn_xF_2$ system. The $K_2Fe_{1-x}In_xCl_5 \cdot H_2O$ sample in

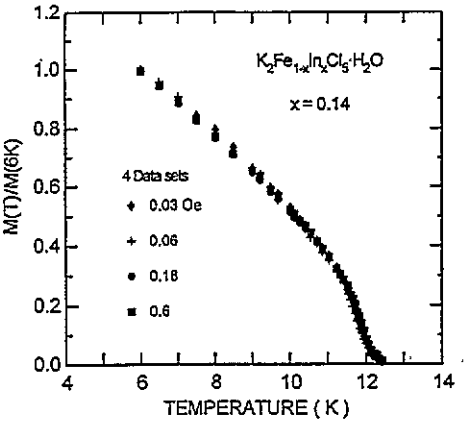

Figure 5. The temperature dependence of the normalized magnetization $M(T)/M(6\text{ K})$ for $x = 0.14$. All four data sets in figure 2 are included in this plot.

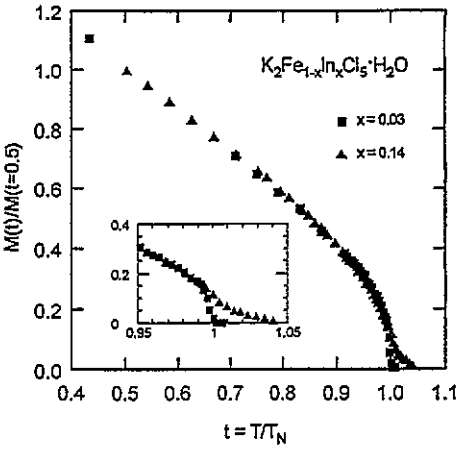

Figure 6. The normalized magnetization as a function of reduced temperature $t = T/T_N$. Both sets of data, for $x = 0.03$ and $x = 0.14$, were taken at 0.6 Oe. In each case M was normalized to its value at $t = 0.5$. The value of T_N for $x = 0.14$ was chosen at the inflection point of M_r against T. In the inset, the region near $t = 1$ is expanded.

figure 7, with $x = 0.10$, is different from the samples in figures 4–6, but its normalized magnetization against t is the same. The results in figure 7 are particularly striking because the only common features of $K_2Fe_{1-x}In_xCl_5{\cdot}H_2O$ and $Mn_{1-x}Zn_xF_2$ are that both are low-anisotropy easy-axis antiferromagnets, and both magnetic ions (Mn^{2+} and Fe^{3+}) are S-state ions with spin $\frac{5}{2}$. The crystallographic structures of the two systems are different, and so are the superexchange paths governing the exchange interactions [14–16].

3.3. Experimental results and data collapse for $K_2Fe(Cl_{1-x}Br_x)_5{\cdot}H_2O$

Similar magnetization measurements were performed on $K_2Fe(Cl_{1-x}Br_x)_5{\cdot}H_2O$ with $x \cong 0.25$, which is a random-bond system. Data were taken for axial fields between 0.008 and 4.1 Oe. The results are shown in figure 8. Here, the thermoremanent magnetization M_r at various values of H_{axial} is plotted as a function of T. The values of M_r were obtained from the raw data for M by using (1). That is, the contribution of $\chi_\parallel H$ to M, which cannot be neglected in this case because M_r is small, was subtracted. Values of $\chi_\parallel$ were obtained from magnetization data at 2 and 4 kOe, as in [3].

It is clear from figure 8 that a TRM exists also for $K_2Fe(Cl_{1-x}Br_x)_5{\cdot}H_2O$, and that this M_r approaches saturation in fields of several Oe. However, the magnitude of M_r, per gram or per mole, is two orders of magnitude smaller than in corresponding random-site samples, e.g., the $K_2Fe_{1-x}In_xCl_5{\cdot}H_2O$ sample in figure 2. Moreover, the temperature dependence of M_r is very different from that found in $K_2Fe(Cl_{1-x}Br_x)_5{\cdot}H_2O$; i.e., with decreasing temperature, M_r first increases, then passes through a maximum, and finally decreases. The normalized M_r against T, for the various values of H_{axial}, is shown in figure 9. Clearly, data collapse is only fair in this case. It is also obvious that the temperature dependence in figure 9 does not agree with that in figures 4–7.

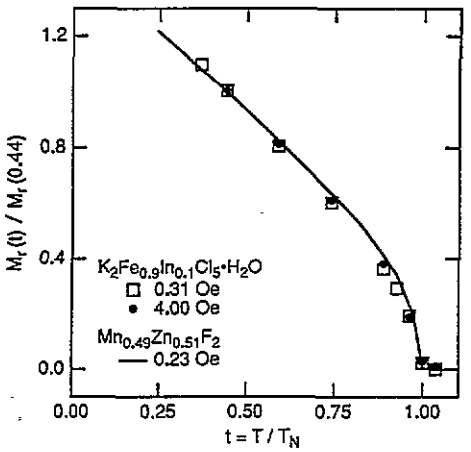

Figure 7. A comparison between the normalized M_r of $K_2Fe_{1-x}In_xCl_5{\cdot}H_2O$ with that in $Mn_{1-x}Zn_xF_2$ [3]. The results for $K_2Fe_{1-x}In_xCl_5{\cdot}H_2O$ are for $x = 0.1$ at two different fields. All data are plotted versus $t = T/T_N$, and are normalized to the value at $t = 0.44$.

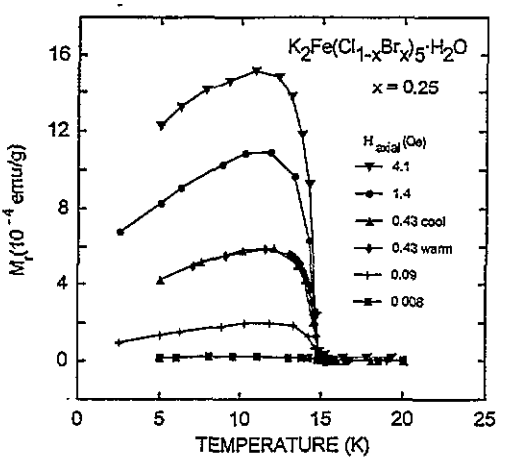

Figure 8. The temperature dependence of the thermoremanent magnetization, M_r, in $K_2Fe(Cl_{1-x}Br_x)_5{\cdot}H_2O$ at several fixed values of the axial field. All data are FC, except at 0.43 Oe, for which both FC and FH data are shown.

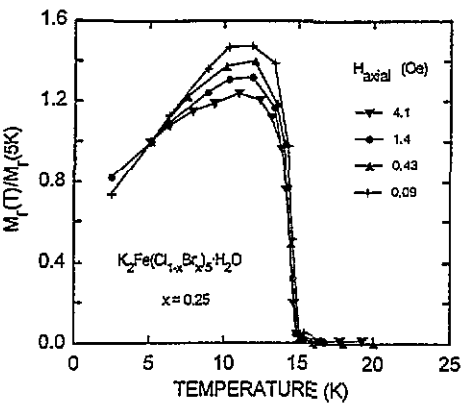

Figure 9. The temperature dependence of the normalized magnetization $M_r(T)/M_r(5\ \text{K})$ for $K_2Fe(Cl_{1-x}Br_x)_5{\cdot}H_2O$, at various axial fields.

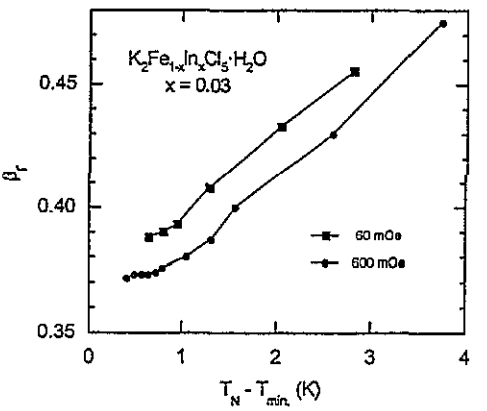

Figure 10. The effective critical exponent β_r as a function of the range $T_N - T_{min}$ used in the fit to (2). These results are for $x = 0.03$. The two curves correspond to data obtained at 0.06 and 0.6 Oe.

3.4. Effective critical exponent β_r for the remanent magnetization

An effective critical exponent β_r was obtained by fitting the temperature variation of M, at fixed H_{axial} and for temperatures just below T_N, to the equation

$$M = A[1 - (T/T_N)]^{\beta_r}. \tag{2}$$

Here, A is a constant, which depends on H_{axial}. Such an analysis was performed only for $K_2Fe_{1-x}In_xCl_5{\cdot}H_2O$, and only for the sample with $x = 0.03$, which had a relatively sharp Néel temperature (see figure 6). The results for β_r, obtained from fits to (2) of data at

0.06 and 0.6 Oe, are shown in figure 10. The abscissa in this figure is the width of the temperature range ($T_N - T_{min}$) covered by the fit. Besides β_r, the constant A and T_N were also treated as fitting parameters. Extrapolation of the results for β_r to zero range give values in the interval from 0.35 to 0.39. These extrapolated values agree with those obtained in the $Mn_{1-x}Zn_xF_2$ system [3]. Because the sublattice magnetization in the $K_2Fe_{1-x}In_xCl_5{\cdot}H_2O$ system has not yet been measured, a direct comparison between our results for β_r and the usual exponent β for the staggered magnetization is not possible. For the $Mn_{1-x}Zn_xF_2$ system the experimental values of β at $H = 0$ are $\beta = 0.35 \pm 0.01$ from nuclear magnetic resonance (NMR) [17], and $\beta = 0.35 \pm 0.03$ and 0.33 ± 0.02 from x-ray scattering [18, 19]. It far from certain that β_r should be equal to β.

3.5. *Field-switching experiments*

All the experiments in the preceding sections followed the FC and FH protocols, i.e., cooling from above T_N in a constant field and then warming in the same field. The procedures used in the field-switching experiments described in the present section were different. The sample was first cooled in an axial field H_1, starting at a temperature above T_N and ending at a temperature T_s below T_N. This initial part of the cycle was identical to that in the FC procedure. After reaching the switching temperature T_s the axial field was switched to H_2 (usually with sign opposite to that of H_1, corresponding to a reversal of field direction). The sample was then cooled in the field H_2 to a temperature well below T_s. Data obtained while cooling after the field switch will be referred to as CAS (cool after switch) data. After reaching the lowest temperature, the sample was heated in the field H_2 to a temperature above T_N. Data obtained while heating in the field H_2 will be called HAS (heat after switch) data. Both CAS and HAS data were always compared to FC results obtained in the field H_1 over the same temperature range. The FC data (with no field switch) were taken separately. Field-switched data were taken only on the $K_2Fe_{1-x}In_xCl_5{\cdot}H_2O$ system.

The main conclusion of the field-switching experiments is that as long as $|H_2 - H_1| \lesssim 1$ Oe, changing the field has no effect on M. That is, CAS and HAS values of M (measured at H_2) are still equal to those obtained with the FC procedure in the field H_1. In other words, M_r is governed by the field H_1 present while cooling through T_N, and is unaffected by the field switch below T_N. Data supporting this conclusion are shown in figure 11. Here, the field was switched from $H_1 = -0.31$ Oe to $H_2 = +0.28$ Oe at a temperature $T_s = 12$ K, which is only slightly below $T_N = 13.4$ K. Similar results were obtained in this sample when the axial field was switched at 12.5 K from $H_1 = -0.08$ to $H_2 = +1.48$ Oe.

When the difference $|H_2 - H_1|$ was much larger than 1 Oe, the CAS and HAS results for M_r in the field H_2 were very different from the FC values at H_1. This is illustrated by the results in figure 12, which are for the same sample as in figure 11. In figure 12 the field was switched at $T_s = 12.5$ K from $H_1 = +0.01$ Oe to $H_2 = -9.74$ Oe. The data shown are actually for M, not for M_r. Because the field H_2 is relatively large, some of the difference between the CAS (or HAS) values of M on one hand and the FC values on the other is due to the term $\chi_\parallel H_{axial}$ in equation (1). Indeed, for temperatures above T_N this the sole reason for the difference between the HAS and FC data. However, this is not the case for temperatures below T_N, where $\chi_\parallel$ decreases with decreasing T. As can be seen in figure 12, below T_s the difference between the HAS (or CAS) values of M and the FC values increases with decreasing T, which is just the opposite behaviour to that of $\chi_\parallel(H_1 - H_2)$. Thus the field switch in this case had a substantial effect on M_r. This conclusion may also be reached by noting that the maximum value of the difference $\chi_\parallel(H_1 - H_2)$ occurs just above T_N. Thus, in figure 12 the much larger difference between the full and the dashed curves when T is well below T_N must be due to the change of M_r.

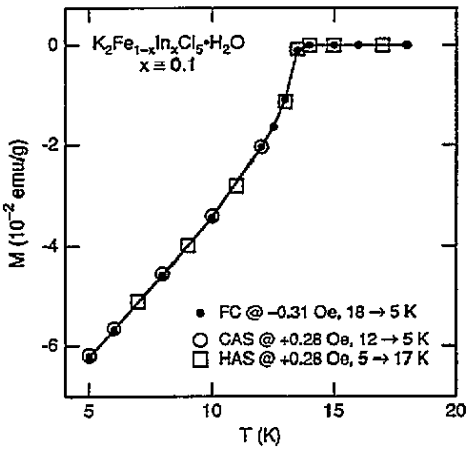

Figure 11. The temperature dependence of M for $x = 0.1$. The solid circles are FC data at $H_1 = -0.31$ Oe. The open circles and squares represent CAS and HAS data, respectively, taken after switching the field at $T_s = 12$ K from H_1 to $H_2 = +0.28$ Oe.

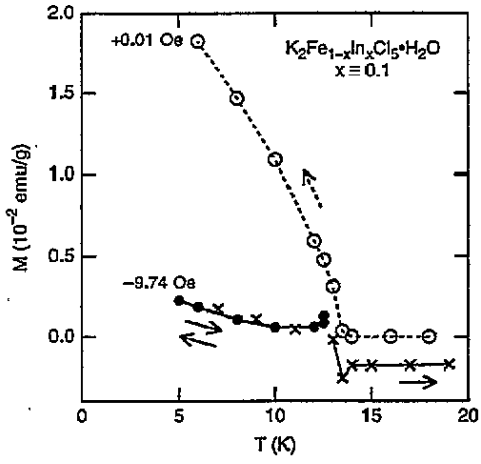

Figure 12. The temperature dependence of M for the same sample as in figure 11, but in this case the field was switched from $H_1 = 0.01$ Oe to $H_2 = -9.74$ Oe at $T_s = 12.5$ K. Open circles are FC data at $H_1 = 0.01$ Oe. The full circles and the × symbols correspond, respectively, to CAS and HAS data at $H_2 = -9.74$ Oe.

An interesting feature in figure 12 is the dip in the HAS value of M just below T_N. Since H_2 is negative, the dip in M corresponds to a peak in M/H. Figure 13 shows a similar behaviour in another sample. Again, the peak in M/H occurs just below T_N. The CAS and HAS data in figure 13 were obtained after a relatively large change of H_{axial}, from +0.012 Oe to −9.0 Oe. The switching temperature was roughly 1 K below T_N. The fact that the difference between the CAS (or HAS) values for M and the corresponding FC values does not decrease as T decreases implies that M_r was significantly affected by the field switch. That is, one cannot attribute the larger FC values of M below T_N solely to the term $\chi_{\parallel}H_{axial}$. Another interesting feature in figure 13 is a slight difference between the HAS and CAS results. This difference grows with increasing T.

3.6. Temperature cycles following cooling in zero field

In another set of experiments the sample was first cooled in zero axial field, starting from above T_N. After reaching a temperature T_m well below T_N, a finite axial field H^* was applied and data were taken in this constant field. In one procedure the sample was always heated in the field H^*, starting at T_m. Data obtained while heating in constant field will be called FHAZFC (field heating after zero-field cooling). This notation is somewhat unusual: it is more common to use the term ZFC to describe such data. However, we feel that the notation FHAZFC emphasizes the fact that the data are actually being taken while heating in a field and not while cooling in zero field. FHAZFC data taken in an axial field H^* were often compared with FC data obtained in the same field. (They were not compared with FC data at $H_{axial} = 0$, which is the field at which the sample was cooled through T_N. One reason is that FC data at $H_{axial} = 0$ give the trivial result $M = M_r = 0$.)

In most cases FHAZFC data were taken up to temperatures somewhat above T_N. However, in some instances the heating in the field H^* was stopped at a 'reversing' temperature T_r below T_N. Subsequently, data were taken while cooling back to T_m and then heating from

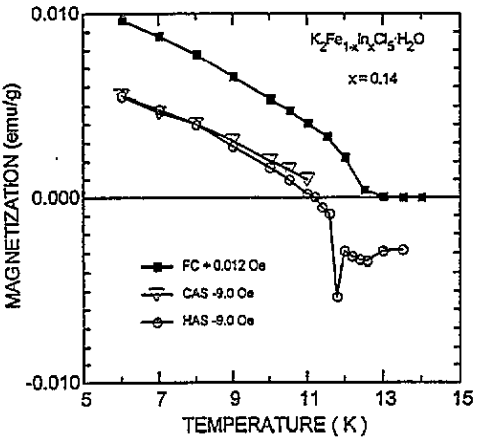

Figure 13. The temperature dependence of M for $x = 0.14$. The solid squares are FC data at $H_1 = 0.012$ Oe. The CAS and HAS data (open triangles and circles, respectively) were taken after switching to $H_2 = -9$ Oe at $T_s = 11.2$ K.

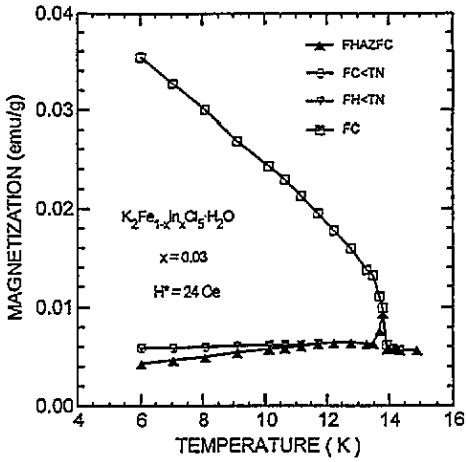

Figure 14. Temperature cycles for $x = 0.03$. After cooling the sample at $H = 0$ (ZFC), an axial field of 24 Oe was applied and FHAZFC data were taken while heating to $T > T_N$ (solid triangles). Cooling from above T_N at 24 Oe results in the FC curve (open squares). The open circles and open triangles correspond to the FC < TN and FH < TN procedures, both carried out at 24 Oe after reversing the temperature sweep at $T_r = 11.2$ K.

T_m, all in the same field H^*. The latter cooling–heating cycle is very different from the normal FC–FH cycle because (i) it starts at $T_r < T_N$, and not above T_N, and (ii) the field H^* was applied below T_N (after cooling in zero field) and not above T_N as in the FC procedure. Data taken while cooling from T_r in constant field will be designated as FC < T_N, while those taken subsequently while heating from T_m will be designated as FH < T_N. This notation is designed to distinguish such data from the usual FC and FH data.

Figure 14 shows data for $x = 0.03$ taken after cooling in zero axial field to $T_m = 6$ K, and then applying an axial field $H^* = 24$ Oe. The FHAZFC data are shown as solid triangles. They exhibit a pronounced peak just below T_N, resembling the peak exhibited by HAS data described previously. A similar peak in FHAZFC data was observed earlier by Ikeda and Kikuta in the $Mn_{1-x}Zn_xF_2$ system [20]. A quantitative analysis of the FHAZFC data in figure 14 indicates that, well below T_N, M is larger than $\chi_{\parallel}H^*$. This means that M_r, as obtained from (1), has increased from the zero value that resulted from cooling in zero field. The increase of M_r is consistent with other results, which show that M_r is affected when the axial field is changed by much more than 1 Oe. Note, however, that the FHAZFC data in figure 14 still lie substantially below the FC curve at the same field (except near the peak, and above T_N). Thus, M_r during the FHAZFC process is merely a fraction of its value during the normal FC procedure at the same field. Only at the peak, which is just below T_n, does the system become 'unfrozen' and capable of attaining the full magnetization response exhibited by the FC curve.

Also shown in figure 14 are FC < TN and FH < TN data. Clearly, these data are above the FHAZFC data at the same field. We will return to this point in section 4.

3.7. Isothermal field cycles

Isothermal field cycles (hysteresis curves) were taken below T_N, both after cooling in zero axial field and after cooling in fields up to several oersted. Some hysteresis cycles employed only low fields, but others extended up to several kilooersted.

Cooling in zero field results in $M = M_r = 0$. If the fields then applied are lower than ~ 1 Oe, the magnetization is reversible and is given by $\chi_\parallel H_{axial}$. As discussed in [3] this result implies that at these low fields M_r is equal to the excess magnetization ΔM.

When much higher fields are applied (e.g., 24 Oe for $x = 0.03$, as in figure 14) the magnetization becomes irreversible, so that when the field is removed some magnetization remains. By definition, the magnetization that remains is the isothermal remanent magnetization (IRM). When much larger fields of more than several kilooersted are applied and removed, the IRM is equal to the saturation value of M_r obtained in FC experiments in fields above ~ 1 Oe.

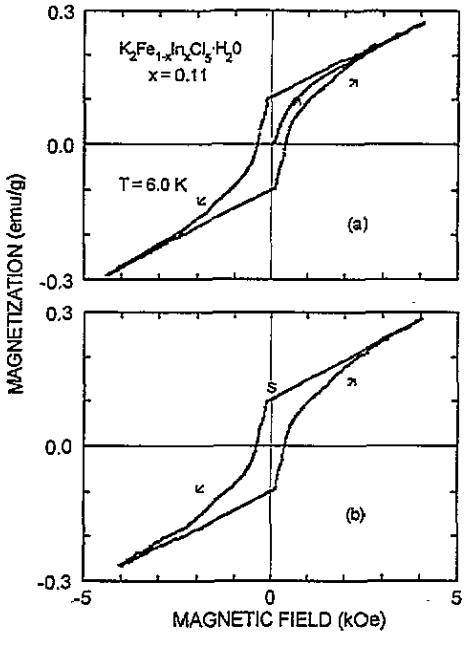

Figure 15. Hysteresis cycles for a sample with $x = 0.11$ taken at $T = 6$ K. In (a) the field cycle is $0 \rightarrow 5$ kOe$\rightarrow 0 \rightarrow -5$ kOe$\rightarrow 0 \rightarrow 5$ kOe$\rightarrow 0$. This cycle is obtained after a ZFC of the sample from above T_N. The cycle in (b) is obtained after cooling the sample in the remanent field of the superconducting magnet. This cycle starts at point S, with a positive value of M. The arrows indicate the direction of the field cycle.

Figure 15(a) shows hysteresis curves obtained after cooling in zero field. The data are for $x = 0.11$ at 6 K. The starting point is $M = H = 0$. As H increases there is a progressive increase of M. This increase resembles the behaviour of systems with spontaneous magnetization when they are magnetized starting from a domain state with $M = 0$. For fields above 5 kOe (not shown), the magnetization curve follows (1) with a constant (saturated) value of M_r. The slope for M versus H in this high-field region is the value of $\chi_\parallel$ in the antiferromagnetic state. When the field is then decreased from a high positive value, M decreases linearly down to $H = 0$ with the same slope $\chi_\parallel$. The magnetization that remains at $H = 0$ is the IRM. It is equal to the value of M_r obtained in FC experiments carried out in fields of ~ 1 Oe. When the direction of H is then reversed, M initially continues to follow the linear behaviour, with a slope $\chi_\parallel$. In figure 15(a) the linear behaviour persists up to negative fields of about 200 Oe. (The field where the linear region ends depends on x and on T, and is the subject of an ongoing investigation.) For

negative fields of larger magnitude, M first decreases rapidly, and then approaches the linear behaviour given by (1) with a constant negative M_r. A subsequent decrease of the field from large negative values leads to a behaviour similar to that observed when the field decreases from large positive values. The full hysteresis curve, except for the initial field increase, is nearly symmetric. Also, the linear regions are reversible, i.e., if the direction of the field sweep is reversed in the middle of a linear region, then the curve is reversible in that region.

Figure 15(b) shows the hysteresis curve for the same sample and temperature, but after cooling in the remanent field of the superconducting magnet, estimated as ~ 1 Oe. The starting point of the isothermal cycle is indicated in the figure by S, and corresponds to a positive M equal to the saturation value of M_r. The field cycle is initiated by applying a negative field of increasing magnitude. The field cycle leads to a magnetization loop that never goes through the origin. This behaviour led us to interpret these results erroneously, in the first paper on this subject [1], as evidence for a monodomain with a spontaneous moment. Comparison of figure 15(a) and (b) shows that the external loops are nearly identical. In particular, the values of the remanent magnetizations, at $H = 0$, for both curves are the same.

4. Discussion

When a 3D easy-axis diluted antiferromagnet is cooled at $H = 0$, from above T_N to $T < T_N$, an equilibrium state with LRO is expected to result, assuming that the material is above the percolation limit [5–7]. This ZFC procedure is the standard method of preparing the system for measurements in the ordered equilibrium state. A subsequent application of a field H will preserve the LRO as long as this field does not drive the system through the boundaries of the antiferromagnetic phase. In this context it is worth noting that most 'ZFC experiments' on real systems are performed in the presence of the remanent field of a superconducting magnet [10, 20, 21]. The magnitude of this remanent field is typically several oersted. We now know that such a remanent field will saturate the low-field remanent magnetization of both $Mn_{1-x}Zn_xF_2$ and $K_2Fe_{1-x}In_xCl_5{\cdot}H_2O$, and presumably also of some other diluted antiferromagnets.

When a 3D diluted antiferromagnet is cooled in an axial field (FC instead of ZFC), the low-temperature *equilibrium* state still has LRO, but this equilibrium state is not achieved. Instead, due to the extremely slow dynamics near the ordering temperature $T_N(H)$ at finite H, the system is trapped in a non-equilibrium microdomain phase [5]. The microdomains are pinned by the RF generated by H. The first question we address is whether the low-field remanent magnetization observed in the present work is associated with the microdomains produced by the RF.

Theoretical treatments of the size and relaxation of the RF-induced domains were given in [5–7]. It was shown that the mean radius R of a domain (for broad domain walls in a 3D system) is proportional to H^{-2}. One model, supported by Monte Carlo simulations [11–13], is that the excess magnetization $\Delta M = M_{FC} - M_{ZFC}$ is concentrated in the walls of the domains [8]. In that model ΔM is proportional to R^{-1} and hence to H^2. Previous experimental studies on $Fe_{0.7}Mg_{0.3}Cl_2$ and $Fe_{0.47}Zn_{0.53}F_2$ [8–10] seem to confirm this predicted field dependence of ΔM. It must be noted, however, that the magnetic fields used in all these previous studies were two to four orders of magnitude higher than those used in the present work. In the present low-field experiments M_r (which is equal to ΔM below ~ 1 Oe) is definitely not proportional to H^2.

A second contribution to ΔM is expected theoretically from the statistically imbalance between the numbers of up and down spins in any given domain. This 'volume contribution' to ΔM is expected to be proportional to H^3 [9]. Estimates indicate that the volume contribution is small compared to the 'surface contribution' from the domain walls [9]. The crucial point, for present purposes, is that both volume and surface contributions increase rapidly with H. This prediction is in clear contrast with the low-field saturation of the remanent magnetization observed in the present work. It thus appears that the present observations at very low fields cannot be explained in terms of H-induced random fields. This means that virtually all previous models for the remanent magnetization in dilute antiferromagnets do not apply to the present observations.

It is known that antiferromagnetic domains exist even at $H = 0$, i.e., in the absence of RF [22]. The possibility that the low-field remanent magnetization is due to such domains was first suggested in [3], although the specific mechanism was not identified. One specific model that was rejected assumed that M_r was due to the imbalance between the numbers of up and down spins in such domains [3]. In this 'DV model' the domains are supposed to be 'frozen' below T_N, in order to explain the field switching experiments.

We briefly repeat the essence of the DV model. Let the number of cation sites on one sublattice in a typical domain be N. Due to the random statistics of replacing Fe by In, one of the sublattices ('majority' sublattice) in each domain has more spins than the other. When the system is cooled through T_N in the presence of a field $\boldsymbol{H}$ along the easy axis, the Zeeman energy favours the configuration in which the majority sublattice has its spins parallel to $\boldsymbol{H}$. As a result, more spins in the sample as a whole are parallel to $\boldsymbol{H}$. This is the origin of the remanent magnetization in this model. The magnitude of the remanent magnetization increases with H because at higher H more domains have their majority-sublattice spins parallel to $\boldsymbol{H}$. The remanent magnetization saturates when H is sufficiently high so that in practically all the domains the majority-sublattice spins are parallel to $\boldsymbol{H}$. It was shown in [3] that at any value of H, M_r in this model is proportional to the sublattice magnetization. Both the observed monotonic increase of M_r with decreasing T (except in the $K_2Fe(Cl_{1-x}Br_x)_5{\cdot}H_2O$ system), and data collapse for a single sample, then follow.

Although the DV model explains some of the experimental results, other observations cast strong doubts on its validity [3]. One difficulty arises when N is estimated and is then used to calculate the energetics of the saturation process. Here we apply the same procedure as in [3] to the sample $K_2Fe_{1-x}In_xCl_5{\cdot}H_2O$ with $x = 0.14$. For that sample the extrapolated value of M_r at $T = 0$ is 1.7×10^{-1} emu g^{-1}, achieved already in a field $H = 1$ Oe. The calculated saturation value for the sublattice magnetization is $M_s = 35$ emu g^{-1}. An estimate for N is then obtained from the relation

$$M_r/M_s \cong [x/N(1-x)]^{1/2} \tag{3}$$

which gives $N = 7 \times 10^3$. This is an unexpectedly small domain at such low magnetic fields. A more serious difficulty arises when we try to account for the fact that saturation of the remanent moment $M_r(T)$ is achieved even at 1 Oe at temperatures just below T_N. For such a saturation to occur we expect that $m_d H/k_B T \geqslant 1$, where m_d is the average net magnetic moment per domain. The latter has the estimated value [3]

$$m_d = [x(1-x)N]^{1/2}\langle\mu\rangle \tag{4}$$

where $\langle\mu\rangle$ is the average magnetic moment per spin. We used the above value of N, a saturation value of 5 Bohr magnetons for $\langle\mu\rangle$, and the temperature dependence of $\langle\mu\rangle$ (which

in this model is the same as that of M_r). This gave $m_d H/k_B T \sim 3 \times 10^{-4}$ at $H = 1$ Oe and $T = 10$ K, which is far too low to account for the observed saturation at this temperature and field.

It should be noted that an imbalance between the numbers of up and down spins in an antiferromagnetic domain can only occur in a random-site system. Thus, the observation of the remanent moment in the random-bond system $K_2Fe(Cl_{1-x}Br_x)_5 \cdot H_2O$ means that at least in that system the effect is not due to such an imbalance.

Other difficulties of the DV model are related to the fact that the T dependence of M_r in $Mn_{1-x}Zn_xF_2$ does not follow closely that of the sublattice magnetization, as predicted by the model [3]. Because there are no data for the T dependence of the sublattice magnetization of $K_2Fe_{1-x}In_xCl_5 \cdot H_2O$, such a comparison cannot be made here.

Although the DV model fails, it is still very likely that the low-field remanent magnetization is associated with low-field domains. Two issues to be addressed are (i) what mechanisms are responsible for the spontaneous magnetization of a domain? and (ii) what factors control the formation of antiferromagnetic domains at low fields? Regarding the origin of the spontaneous moment, one possibility is a surface magnetization in domain walls [3]. Another possibility is magnetization in the bulk of a domain due to the piezomagnetic effect [21]. As for the formation of domains at low fields, it may be facilitated by site disorder, e.g., the substitution of In for Fe. The reason for this is the lower cost in exchange energy when the domain wall passes through a non-magnetic cation. A larger number of domains should increase M_r because both the surface to volume ratio and the average random strain increase as the domains become smaller. This may explain why a larger M_r was observed in $K_2Fe_{1-x}In_xCl_5 \cdot H_2O$ than in $K_2Fe(Cl_{1-x}Br_x)_5 \cdot H_2O$.

The hysteresis curves in figure 15 are similar to those observed in ferromagnets and other systems that exhibit domains, and a spontaneous magnetization in each domain. For example, the magnetization curve in figure 15(a), which starts at $M = H = 0$, resembles the magnetization curve of a ferromagnet that has been cooled in zero field. This similarity suggests that in the present case too domains are formed when the sample is cooled in zero (or low) field and that a spontaneous magnetization exists in each domain (or in the walls). The hysteresis curves in figure 15 then corresponds to a superposition of two processes: the gradual alignment of the spontaneous magnetization of the domains, and the ordinary contribution $\chi_\parallel H$ from the antiferromagnetic phase. The data in figure 15 show that at $T = 6$ K a field of about 3 kOe or so is required to saturate the spontaneous moment. This is a much higher field than that required to saturate the moment in FC experiments.

The ZFC procedure is generally accepted as the correct method of preparing the diluted system in the LRO equilibrium state. Subsequent heating in a field (FHAZFC) and then cooling in the same field from a temperature T_r below T_N (FC < TN) should give the same results for M. That is, the magnetization at constant H following ZFC (and avoiding heating through T_N) is expected to be reversible. In contrast, actual experiments in real systems [9, 10] and Monte Carlo simulations [12] reveal an irreversible behaviour: the magnetization in the FC < TN part of the cycle is higher than that in the FHAZFC portion of the cycle. In the Monte Carlo simulations the cooling in the FC < TN part of the cycle was started at $0.8T_N$, and the irreversibility was attributed to 'small spin cluster flipping that creates a domain type state without destroying the LRO'. Figure 14 shows that a similar irreversible behaviour (the difference between FHAZFC and FC < TN) is also seen in the present experiments at low fields. Apparently, when the temperature sweep is reversed not too far below T_N, a field of even ~ 10 Oe succeeds in flipping the magnetic moments of some of the domains, presumed to be present even at $H_{axial} = 0$. Thus, a larger net magnetization is observed in the FC < TN part of the cycle.

One surprising feature is the T dependence of M_r in $K_2Fe(Cl_{1-x}Br_x)_5{\cdot}H_2O$ (see figure 8). In this sample M_r first increases but then decreases with decreasing T, in contrast to the monotonic growth of M_r with decreasing T in $K_2Fe_{1-x}In_xCl_5{\cdot}H_2O$ and Mn_{1-x} Zn_xF_2. At first sight it may seem that this difference arises because $K_2Fe(Cl_{1-x}Br_x)_5{\cdot}H_2O$ is a random-bond system whereas the other two are random-site systems. However, preliminary measurements on $(K_{1-x}Rb_x)_2FeCl_5{\cdot}H_2O$, which is also a random-bond system, show a monotonic increase of M_r with decreasing T. It is noteworthy that a temperature dependence similar to that in $K_2Fe(Cl_{1-x}Br_x)_5{\cdot}H_2O$ was observed in $Fe_{1-x}Zn_xF_2$ [9], but that observation was made at much higher fields where random fields are presumed to be important.

5. Conclusions

The low-field remanent magnetization in $K_2Fe_{1-x}In_xCl_5{\cdot}H_2O$ is very similar to that in $Mn_{1-x}Zn_xF_2$, except that M_r in $K_2Fe_{1-x}In_xCl_5{\cdot}H_2O$ (in emu mol^{-1} or emu g^{-1}) is up to two orders of magnitude larger. Hysteresis cycles, such as those in figure 15, suggest that at low fields the samples consist of domains, each having spontaneous net magnetization in its volume or in its walls. A definitive proof for such domains is still lacking, however. The origin of the spontaneous domain magnetization, which is presumed to be responsible for the remanent magnetization, is not known with certainty, but domain-wall magnetization [3] or a piezomagnetic moment [21] are suspected. The usual explanation of the remanent magnetization in terms of random fields generated by H definitely fails.

The fact that the t dependence of the normalized M_r in all $K_2Fe_{1-x}In_xCl_5{\cdot}H_2O$ samples is the same, and that it agrees with that in $Mn_{1-x}Zn_xF_2$, suggests that the low-field remanent magnetization has a universal character. Since this novel universal phenomenon is still not fully understood, further theoretical and experimental work is needed.

Acknowledgments

The work at the University of São Paulo (USP) was supported by CNPq and by FAPESP under grant 92/0845-2. The work at Tufts University was supported by NSF grant DMR-9219727. The equipment in the Magnetometry Facility at Tufts was donated by the W M Keck Foundation. The work at the University of Zaragoza was supported by CICYT grant MAT91-681. The cooperation between Tufts and USP is supported by NSF grant INT-9216424 and CNPq. The cooperation between the University of Zaragoza and USP is supported by the Programa de Cooperacion Iberoamericana and CCInt-USP.

Note added in proof. The magnetic space group for the pure compounds $K_2FeCl_5{\cdot}H_2O$ and $Rb_2FeCl_5{\cdot}H_2O$ has been recently found to be $Pn'm'a'$ (M Gabás *et al* to be published). The magnetic Laue group of $Pn'm'a'$ is $m'm'm'$ which by symmetry is not consistent with piezomagnetism.

References

[1] Paduan-Filho A, Barbeta V B, Becerra C C, Gabas M and Palacio F 1992 *J. Phys.: Condens. Matter* **4** L607
[2] Fries T, Shapira Y, Paduan-Filho A, Becerra C C and Palacio F 1993 *J. Phys.: Condens. Matter* **5** L107
[3] Fries T, Shapira Y, Paduan-Filho A, Becerra C C and Palacio F 1993 *J. Phys.: Condens. Matter* **5** 8083
[4] Fishman S and Aharony A 1979 *J. Phys. C: Solid State Phys.* **12** L729
[5] Villain J 1984 *Phys. Rev. Lett.* **52** 1543
[6] Bruinsma R and Aeppli G 1984 *Phys. Rev. Lett.* **52** 1547
[7] Nattermann T and Vilfan I 1988 *Phys. Rev. Lett.* **52** 223
[8] Leitao U A and Kleemann W 1987 *Phys. Rev.* B **35** 8696
[9] Pollak P, Kleemann W and Belanger D P 1988 *Phys. Rev.* B **38** 4773
[10] Leitao U A, Kleemann W and Ferriera I B 1988 *Phys. Rev.* B **38** 5220
[11] Yoshikawa H and Belanger D P 1984 *Phys. Rev.* B **30** 5220
[12] Novak U and Usadel K D 1989 *Phys. Rev.* B **39** 2516
[13] Grest G S, Soukoulis C M and Levin K 1986 *Phys. Rev.* B **33** 7659
[14] Carlin R L and Palacio F 1985 *Coord. Chem. Rev.* **65** 141
[15] De Jongh L J and Miedema A R 1974 *Adv. Phys.* **23** 154
[16] Puertolas J A, Navarro R, Palacio F, Bartolome J, Gonzalez D and Carlin R 1985 *Phys. Rev.* B **31** 516
[17] Dunlap R A and Gottlieb A M 1981 *Phys. Rev.* B **23** 6103
[18] Hill J P, Feng Q, Birgeneau R J and Thruston T R 1993 *Z. Phys.* B **92** 285
[19] Thruston T R, Peters C J, Birgeneau R J and Horn P M 1988 *Phys. Rev.* B **37** 9559
[20] Ikeda H and Kikuta K 1983 *J. Phys. C: Solid State Phys.* **16** 1445
[21] Kushauer J, Kleemann W, Mattsson J and Nordblad P 1994 to be published
[22] Farztdinov M M 1965 *Sov. Phys.–Usp.* **7** 855